



The Study of Mapping Strategies Between the Excitators of the Single-Reed Woodwind and the Bowed String

Song Wang¹, Marcelo M. Wanderley², and Gary Scavone¹

¹ Centre for Interdisciplinary Research in Music Media and Technology

² Schulich School of Music, McGill University, Montreal H3A 1E3

Abstract. Mapping is one of the most important components in digital musical instruments. There have been many works on "longitudinal" mapping strategies from the input device to the sound synthesizer. Such mapping can be considered longitudinal because the mapping direction is in line with the information transfer direction. However, less research focuses on "transversal" mappings among input devices or sound synthesizers. In this paper, a transversal mapping strategy is explored between the excitators of bowed strings and single-reed woodwinds which aims to allow more natural use of a given controller to play the sound of another family of instruments. A three-layer mapping structure, namely the playing layer, the mathematical layer, and the physical layer, is built. The mappings in different layers are generated based on the analogy of the mathematical models of two excitators in the mathematical layer. As a result, in the playing layer, the bowing force and the bowing speed of the string instrument are mapped to the lip force and the mouth pressure of a single-reed woodwind, respectively. In the physical layer, the string velocity and the friction force at the bowed point are mapped to the acoustic pressure and the volume velocity in the mouthpiece, respectively. Finally, a Yamaha WX5 wind controller is used to drive the digital waveguide string model. Two different mapping strategies between the lip force and the bowing force are tested and the results are discussed.

Keywords: Mapping, Excitator, Digital Musical Instrument, Single-reed instrument, Bowed string

1 Introduction

Mapping between the input device and the synthesis device is one of the keys to the digital musical instrument [1, 2]. As the link connecting the controller and the synthesizer, the mapping defines a pathway that the input information follows to flow toward the output, which builds an implicit bond between the player's gesture and the sound output. Traditionally, mappings are used to describe the relationship between two sets of parameters. Different mapping techniques have been introduced to make the instrument more controllable, such

as neural networks [3–6], interpolation [7–9] and abstract parameters and multi-layered mapping [10, 11]. However, most of previous studies focus on the longitudinal mapping from the input device to the synthesis device with a typically unidirectional flow of information. In this paper, we propose to extend mappings to transversal mappings among input devices or synthesis devices.

Input devices specifically designed for a particular type of music may not work very well to control other families of instruments. The same issue happens to the synthesis device who may work well only when its controlled by a certain type of controllers. In contrast with longitudinal mappings, the transversal mappings build a link among the same category of devices, aiming to extend the applicability of the input device and increase the adaptivity of the synthesis device. A schematic comparison between two kinds of mappings is shown in Fig. 1.

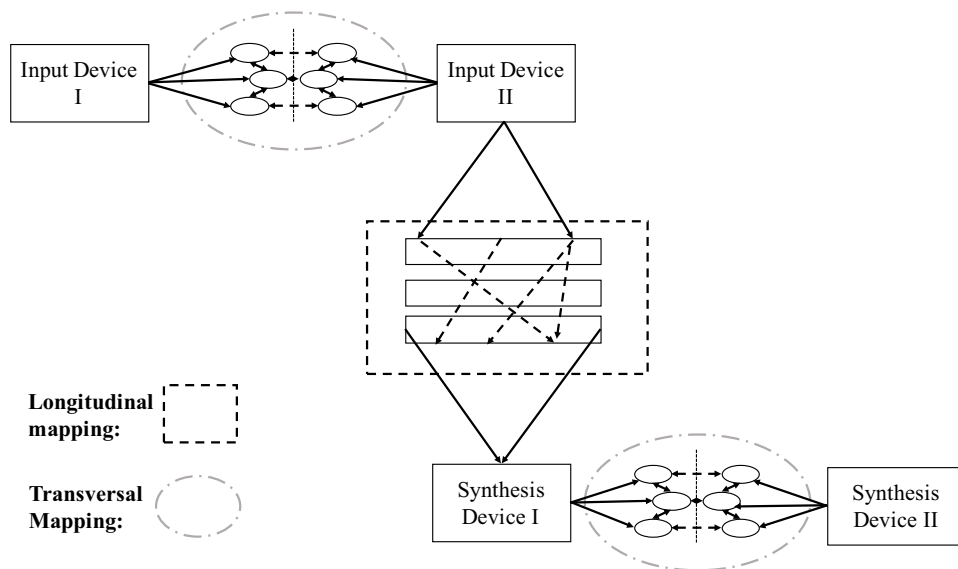


Fig. 1: A schematic view of the longitudinal and transversal mappings

In this paper, a special case of the transversal mapping is studied by exploring the mapping strategies between the excitators of single-reed woodwinds and bowed strings. Using the mapping strategies built in this paper, a wind controller can control the sound synthesizer of a bowed string, and vice versa. This paper is organized as follows: in Section 2, a three-layer mapping structure is proposed and applied to mapping between a bowed string and single-reed woodwinds. A preliminary experiment is conducted in the same Section, using a Yamaha WX5 wind controller to drive a digital waveguide bowed string model. Possible extensions and different interpretations of the mapping are discussed in Section 3. Finally, the conclusion is given in Section 4.

2 Mapping between the bowed strings and the single-reed woodwind

2.1 Three-layer mapping structure

The key to the transversal mapping between two different instruments is to map their playing parameters. However, because of the underlying complex physics, it is not straightforward to directly connect one set of playing parameters to another. In order to solve this problem, a three-layer mapping structure is proposed with three different mapping levels: the *playing layer* (playing parameters), the *mathematical layer* (mathematical models), and the *physical layer* (physical variables). As shown in Fig. 2, mapping on the mathematical layer is first based on the analogy of mathematical models between two instruments, which is shown as the solid line across instruments. Based on different mathematical models, the playing parameters and the physical variables are extracted as two separated layers. The mapping between the playing parameters or the physical variables of different instruments are determined by the role they play in their own mathematical model, shown as dashed lines across instruments. For example, both the bowing velocity in the string model and the mouth pressure in the single-reed model work as the energy source of the system, which makes it obvious to map them to each other.

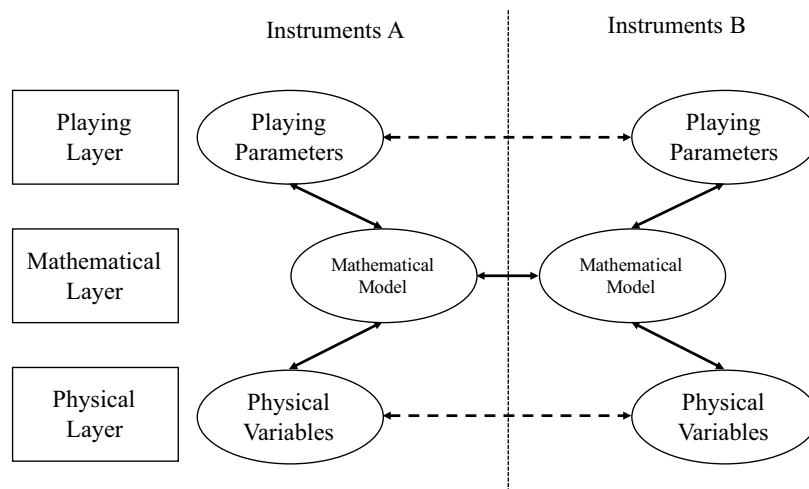


Fig. 2: Three-layer structure of mapping between two different musical instruments

In the next session, the generic mathematic model for self-sustained instruments will be introduced. The bowed string model, single-reed model and their mapping detail will then be discussed.

2.2 Mathematical models and mapping

Generic model Both bowed strings and single-reed woodwinds are classified as self-sustained musical instruments. As shown in Fig. 3, self-sustained musical instruments can generally be decomposed into a nonlinear excitator and a linear resonator. In the mathematical layer of the three-layer mapping structure, we take the excitator mathematical model as the mapping object instead of taking the whole instrument model. This is because the nonlinear excitator, sitting in between the player and the resonator, works as an information exchanger. It dominates sound generation by turning the continuous DC energy source provided by the player into an AC oscillation that excites the resonator. Hence, the excitator mathematical model involves both playing and physical variables, which makes it the best candidate to study mapping.

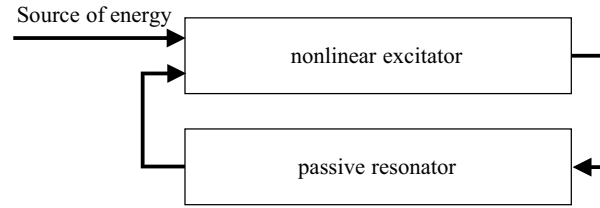


Fig. 3: Block diagram of a generic model for self-sustained instruments

Bowed string model The interaction of the bow and the string is usually considered as the stick-slip motion. The model proposed by Weinreich and Causé [12] is used here. In this model, the contact area between the bow and the string is assumed as a point. The relationship between the friction force f and the velocity difference $\Delta v = v_b - v_s$ between the bow and the string is given by:

$$f = F_b \left(\frac{\Delta v}{v_0} \right) \left[1 + \left(\frac{\Delta v}{v_0} \right)^2 \right]^{-1}, \quad (1)$$

where F_b is the bowing force, v_0 is a control parameter, v_b is the bowing velocity and v_s are the string velocity at the bowing point.

The friction force f as a function of the velocity difference Δv is shown in Fig. 4 with $F_b = 0.15 \text{ N}$ and $v_0 = 0.05 \text{ m/s}$.

Single-reed woodwind model For single-reed instruments, the nonlinearity is depicted by the relationship between the airflow rate in the mouthpiece u and the difference $\Delta p = p_m - p$ between the mouth pressure p_m and the mouthpiece pressure p . In this model, the nonlinear mechanism is assumed to be localized at the entrance of the mouthpiece chamber or the pipe resonator. Based on the

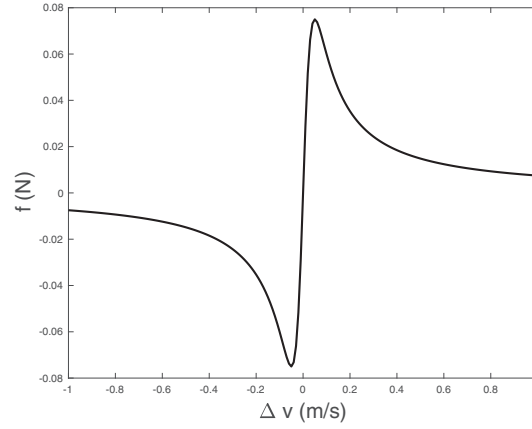


Fig. 4: Friction force in terms of the velocity difference

Bernoulli equation, the relationship is shown as:

$$u = S \sqrt{\frac{2|\Delta p|}{\rho}} \text{sign}(\Delta p), \quad (2)$$

where ρ is the density of the air and $S = wH$ is the cross-section area depending on the width of the reed channel w and the reed tip opening height H . However, when the pressure difference Δp is larger than a closing pressure p_M , the reed will touch the lay of the mouthpiece so that the channel will be closed ($H = 0$) and the airflow rate will be zero ($u = 0$). To keep things simple, the reed is modeled as an ideal spring without damping and inertia. The opening height is given by

$$H = \begin{cases} H_0 - \frac{\Delta p}{K}, & \text{for } p \leq p_M \\ 0, & \text{for } p > p_M \end{cases} \quad (3)$$

where K is the stiffness of the reed and $p_M = KH_0$.

Combining Eqs. 2 and 3, we get:

$$u = \begin{cases} w[H_0 - \frac{\Delta p}{K}] \sqrt{\frac{2|\Delta p|}{\rho}} \text{sign}(\Delta p), & \text{for } p \leq p_M \\ 0, & \text{for } p > p_M, \end{cases} \quad (4)$$

which is further simplified as

$$u = \begin{cases} u_A \left(1 - \frac{\Delta p}{p_M}\right) \sqrt{\frac{\Delta p}{p_M}}, & \text{for } p \leq p_M \\ 0, & \text{for } p > p_M, \end{cases} \quad (5)$$

where

$$u_A = w \sqrt{\frac{2KH_0^3}{\rho}}. \quad (6)$$

The nonlinear characteristic of this equation is shown in Fig. 5 with $w = 12$ mm, $H_0 = 0.3$ mm, $K = 188$ hPa/mm.

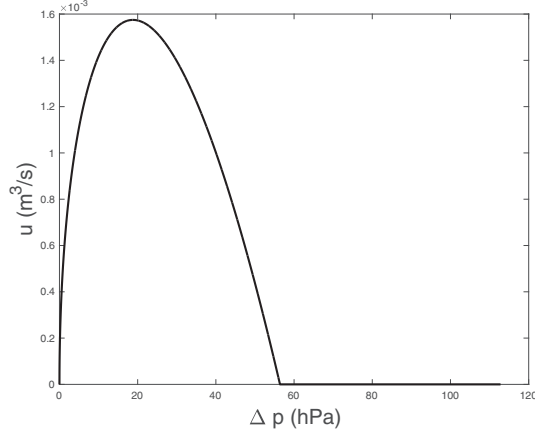


Fig. 5: The function of the flow rate in terms of the pressure difference

In previous research by Ollivier *et al.* [13], the embouchure flow u_A is taken as a playing parameter. However, u_A depends on multiple parameters like the tip opening H_0 and the reed stiffness K . Furthermore, such a parameter is not consciously and directly controlled by the player, and is unlikely to be taken as a playing parameter. Instead, the lip force F_{lip} acting on the reed is taken as the substitute playing parameter in this paper. The way to replace u_A by F_{lip} in the mathematical model is discussed below.

Based on the reed instrument mouthpiece model presented by Avanzini and van Walstijn [14, 15], the lip force influences the damping, stiffness, and also the rest opening height of the mouthpiece channel. Because the damping of the reed is not considered here, only the reed stiffness K and the reed rest opening height H_0 are taken into consideration as functions of lip force F_{lip} . Again, in order to keep things simple, instead of using the reed-mouthpiece-lip interaction model, linear functions built from the measurement data [16] are derived. Based on the data provided by Dalmont *et al.* [16], H_0 and $1/K$ as functions of F_{lip} are shown in Fig. 6.

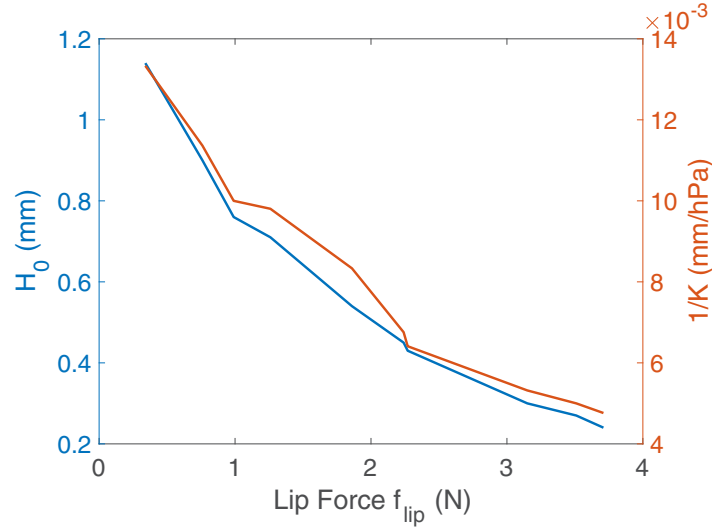
A linear function is used to fit these relationships:

$$H_0 = -aF_{lip} + b, \quad (7)$$

$$\frac{1}{K} = -cF_{lip} + d, \quad (8)$$

where $a = 0.2426$, $b = 1.0614$, $c = 0.0024$ and $d = 0.0130$.

Substituting Eqs. 7 and 8 into Eq. 4, we get:

Fig. 6: H_0 and $1/K$ as functions of $F_{lip}h$

$$u = \begin{cases} [-F_{lip}(a + c\Delta p) + (b + d\Delta p)] w \sqrt{\frac{2|\Delta p|}{\rho}} \text{sign}(\Delta p) & \text{for } p \leq p_M \\ 0 & \text{for } p > p_M \end{cases} \quad (9)$$

where F_{lip} is successfully extracted as an independent variable in the model.

Mapping The three-layer mapping between the bowed string and the single-reed woodwind excitations is shown in Table 1.

In the mathematical layer, the friction force equation and the Bernoulli equation are used to model the bowed string and the single-reed mouthpiece systems, respectively. Based on the analogy of these two sets of equations, the mappings in the physical layer and playing layer are built.

Table 1: Mapping between the excitations of bowed string and single-reed instruments

Mapping Layer	Bowed strings	Single-reed Instruments
physical layer	string velocity v at the bowed point friction force f at the bowed point	acoustic pressure p inside the mouthpiece volume velocity u in the mouthpiece
mathematical layer	friction force equation	Bernoulli equation
playing layer	bowing speed v_b bowing force F_b	pressure inside the mouth p_m lip force F_{lip}

Within the playing layer, the bowing speed v_b is mapped to the pressure in the mouth p_m as they generate energy sources in a similar way. In the bowed string instrument, a non-zero bowing speed leads to the friction between the bow and the string, which in turn provides the source of the velocity wave. Similarly, in the single-reed woodwind, the non-zero mouth pressure forces the air to pass through the reed channel and causes the reed to vibrate, which is the primary source of the pressure fluctuation. On top of the v_b - p_m pair, the lip force F_{lip} is directly mapped to the bowing force F_b . Despite the same physical meaning and unit of F_{lip} and F_b as forces, the lip force and the bowing force have the opposite influence on their physical models. In the bowed string model, a larger F_b results in a larger friction force, which increases the string velocity signal and leads to a louder sound. However, for a single-reed woodwind, as shown in the Eq. 9, a larger F_{lip} makes the u_A smaller, which lowers the sound amplitude. This effect is also explained by previous research and measurements by Almeida and colleagues [17]. Players will loosen their lip pressure for a louder sound or larger dynamics. From the clarinetist point of view, the increasing of the lip force should correspond to a decreasing of the bowing force. However, for a violinist or non-clarinetist, it is obvious to make a positive correlative mapping between these two different forces. Both positive and negative correlative mapping strategies are explored and discussed in the next section.

In the physical layer, the string velocity v at the bowing point is mapped to the acoustic pressure p inside the mouthpiece. Both of them can be used as the physical variables in the physical modeling of the resonator system [18]. In addition, the transverse friction force f is mapped to the volume velocity u inside the mouthpiece. These mappings also lead to a direct link between the instantaneous admittance $Y = v/f$ and impedance $Z = p/u$, which can be taken to describe the characteristics of the bowed string and the woodwind excitators, respectively.

2.3 Mapping experiments

In this section, a Yamaha WX5 wind controller is used to drive a bowed string digital waveguide (DWG) model. The MIDI information of the breath pressure and lip force is provided by the WX5 and taken as the input to the DWG model. The bowed string model is implemented in the Synthesis ToolKit (STK) [19] and packaged as a MAX/MSP object³. The interaction between the bow and the string is implemented by the "bow table" that is generated by Eq. 1.

Based on the mapping strategy discussed in the previous section, the mouth pressure is mapped to the bowing speed, and the lip force is mapped to the bowing force. As discussed earlier, the lip force can be mapped to the bowing force in two different ways so that two experiments are conducted, correspondingly.

In the first case, lip force is positively correlated to the bowing force. As the lip force increases, the sound gets louder, as well as the friction noise. In such a case, the control of the sound is easy and obvious. In the second experiment,

³ See <https://github.com/Cycling74/percolate>.

the lip force is negatively correlated to the bowing force except for the initial state when lip force is zero. The zero lip force of the wind controller corresponds to the off-string bowing status in the bowed string model, which represents a zero bowing force. However, when the player starts to bite the mouthpiece, even very softly, the system will generate a large bowing force and make it very easy to generate sound. Such a mapping will require more and more pressure to generate noiseless sound with the increasing lip force. The negatively correlated mapping makes the instrument harder to control, but in the meanwhile, makes it possible to play the bowed-string synthesizer as if one was playing a real clarinet. However, the embouchure is not exactly the same as the one used to play the real clarinet. This is mainly due to the linear mapping from the MIDI information of the WX5 to the bowing force, which could be improved in the future by introducing a nonlinear relationship.

3 Discussion

3.1 Mathematical model analogy

The key to the three-layer mapping between the bowed string and the single-reed woodwind is the mathematical model analogy. As mentioned by Ollivier et al. [13], the synthesis models have to be simple enough for comparison. Too many parameters of a model will make the analogy impossible even though there are several potential improvements to the current analogy and mapping.

First, a better lumped model of the single-reed woodwind could improve the mapping. As discussed above, the analogy between the mouthpiece and bowed string is based on the similarity between the pressure-flow and the stick-slip characteristics. In the present single-reed woodwind model, the volume velocity is set to zero when the pressure difference Δp is larger than the closing pressure p_M . In the paper by Walstijn and Avanzini [15], a different lumped model is proposed, which generates a more realistic u - Δp relationship by introducing the pressure-dependent stiffness. This model can make the two instrument characteristics more similar to each other as compared in Fig. 7.

Second, the hysteresis is an important effect that happens in both systems due to the characteristic of the reed and the string. As shown in Fig. 8, the two hysteresis effects captured by a complete coupled single-reed woodwind system [20] and the bowed-string model by Schumacher *et al.* [21] resembles each other. Such an analogy of hysteresis deserves a further study and test.

Third, in the current mapping experiment, the playing parameters of the single-reed instrument come directly from the wind controller. So the mapping is from the MIDI number of the single-reed instrument playing parameters to the physical value of the bowed-string playing parameters. However, more physically meaningful mappings can be made by considering the oscillation and extinction thresholds of playing parameters of both instruments. Such a threshold can be based on either modeling or measurement results.

Finally, friction noise is one of the essential elements that determines the naturalness of the sound. The noise is controlled by the bowing force and mouth

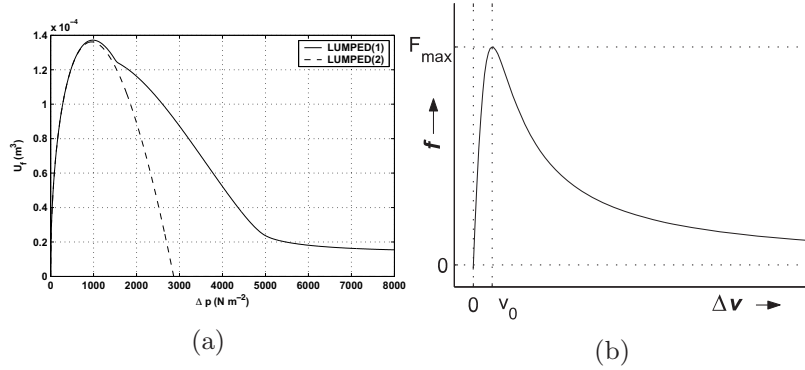


Fig. 7: A basic characteristic of (a) the reed mouthpiece model (LUMPED(1) is the improved model) [15] and (b) the bowed string model [13].

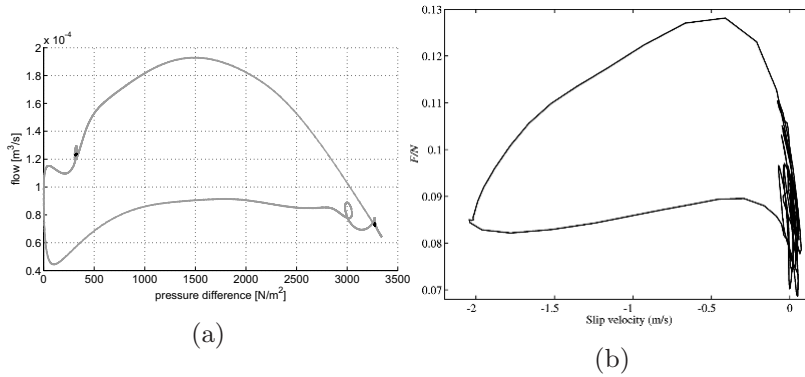


Fig. 8: Hysteresis characteristics of (a) the reed mouthpiece model [20] and (b) the bowed string model [21].

pressure in the bowed string model and the single-reed model, respectively. However, the bowing force and the mouth pressure have no relationship with each other in the current mapping, so the noise of the bowed string might not be well controlled by a wind controller. A different mapping strategy is needed for better control of the noise, which may result in either a convergent or divergent mapping instead of the simple one-to-one mapping [22].

3.2 Discussion on the three-layer mapping structure

In this paper, the three-layer structure mapping is applied between the bowed string and the single-reed woodwind. In contrast to longitudinal mappings, this transversal mapping builds the relationship between the objects of the same category. However, both the input device and the synthesis device are involved in the three-layer mapping. So, this three-layer transversal mapping can also be interpreted as a part of the longitudinal mapping structure, being taken as an implicit mapping layer between the input device and the synthesis device.

Interestingly, the three-layer structure can be explained from both the system point of view and the functional point of view [23]. In terms of the system point of view, the output of the three-layer mapping is the mapping between two sets of parameters of different instruments, i.e., the playing parameter mapping in the playing layer and the physical variable mapping in the physical layer. In addition, these outer layer mappings are all based on the mathematical model analogy that can be considered as the mapping between functions from the functional point of view. In conclusion, the three-layer mapping between the bowed string and the single-reed woodwind has dual characteristics. It can be interpreted as both a transversal mapping and a longitudinal mapping. For the latter case, the mapping can be explained from both the system and functional point of views, which is attributed to the three-layer structure.

4 Conclusions

In this paper, a three-layer structure is proposed to study the mapping between the bowed string and single-reed woodwind. The mathematical model analogy in the mathematical layer provides a direct link between different instrument excitators. Based on the mapping in the mathematical layer, the playing parameters and physical variables are mapped in the playing layer and the physical layer, respectively. Based on such mapping, a Yamaha WX5 wind controller is used to drive the bowed string model. Two different strategies are tested, which provides a preliminary validation of the current mapping. When using positively correlated force mapping, the control is obvious and easy while counter-intuitive to wind performers. However, negatively correlated force mapping may provide more realistic experiences. Furthermore, the limitation and extensions of the current mapping strategies are discussed. Finally, the three-layer structure mapping is successfully interpreted from both the system point of view and the functional point of view.

References

1. Andy Hunt and Marcelo M Wanderley. Mapping performer parameters to synthesis engines. *Organised sound*, 7(02):97–108, 2002.
2. Eduardo Reck Miranda and Marcelo M Wanderley. *New digital musical instruments: control and interaction beyond the keyboard*, volume 21. AR Editions, Inc., Madison, WI, USA, 2006.
3. Matthew Lee and David Wessel. Connectionist models for real-time control of synthesis and compositional algorithms. In *Proceedings of the International Computer Music Conference*, pages 277–277, San Jose, 1992.
4. Sidney S Fels and Geoffrey E Hinton. Glove-talk: A neural network interface between a data-glove and a speech synthesizer. *IEEE transactions on Neural Networks*, 4(1):2–8, 1993.
5. Arshia Cont, Thierry Coduys, and Cyrille Henry. Real-time gesture mapping in pd environment using neural networks. In *Proceedings of the International Conference on New Interfaces for Musical Expression*, pages 39–42, London, 2004.

6. Chris Kiefer. Musical instrument mapping design with echo state networks. In *Proceedings of the International Conference on New Interfaces for Musical Expression*, pages 293–298, London, 2014.
7. Camille Goudeseune. Interpolated mappings for musical instruments. *Organised Sound*, 7(02):85–96, 2002.
8. Ross Bencina. The metasurface: applying natural neighbour interpolation to two-to-many mapping. In *Proceedings of the International Conference on New Interfaces for Musical Expression*, pages 101–104, Vancouver, 2005.
9. Martin Marier. Designing mappings for musical interfaces using preset interpolation. In *Proceedings of the International Conference on New Interfaces for Musical Expression*, Ann Arbor, 2012.
10. Marcelo M Wanderley, Norbert Schnell, and Joseph Rován. Escher-modeling and performing composed instruments in real-time. In *SMC'98 Conference Proceedings. 1998 IEEE International Conference on Systems, Man, and Cybernetics (Cat. No. 98CH36218)*, volume 2, pages 1080–1084, San Diego, 1998.
11. Andy Hunt, Marcelo M Wanderley, and Ross Kirk. Towards a model for instrumental mapping in expert musical interaction. In *Proceedings of the International Computer Music Conference*, Berlin, 2000.
12. Gabriel Weinreich and René Causse. Elementary stability considerations for bowed-string motion. *The Journal of the Acoustical Society of America*, 89(2):887–895, 1991.
13. S Ollivier, J-P Dalmont, and J Kergomard. Idealized models of reed woodwinds. Part I: Analogy with the bowed string. *Acta acustica united with acustica*, 90(6):1192–1203, 2004.
14. Federico Avanzini and Maarten van Walstijn. Modelling the mechanical response of the reed-mouthpiece-lip system of a clarinet. Part I. A one-dimensional distributed model. *Acta Acustica united with Acustica*, 90(3):537–547, 2004.
15. Maarten van Walstijn and Federico Avanzini. Modelling the mechanical response of the reed-mouthpiece-lip system of a clarinet. Part II: A lumped model approximation. *Acta Acustica united with Acustica*, 93(3):435–446, 2007.
16. Jean-Pierre Dalmont and Cyrille Frappe. Oscillation and extinction thresholds of the clarinet: Comparison of analytical results and experiments. *The Journal of the Acoustical Society of America*, 122(2):1173–1179, 2007.
17. André Almeida, David George, John Smith, and Joe Wolfe. The clarinet: How blowing pressure, lip force, lip position and reed "hardness" affect pitch, sound level, and spectrum. *The Journal of the Acoustical Society of America*, 134(3):2247–2255, 2013.
18. Julius O Smith. Physical modeling using digital waveguides. *Computer music journal*, 16(4):74–91, 1992.
19. Perry R Cook and Gary Scavone. The synthesis toolkit (STK). In *Proceedings of the International Computer Music Conference*, pages 164–166, Beijing, 1999.
20. Vasileios Chatziioannou and Maarten van Walstijn. Estimation of clarinet reed parameters by inverse modelling. *Acta Acustica united with Acustica*, 98(4):629–639, 2012.
21. Robert T Schumacher, S Garoff, and J Woodhouse. Probing the physics of slip-stick friction using a bowed string. *The Journal of Adhesion*, 81(7-8):723–750, 2005.
22. Joseph Butch Rován, Marcelo M Wanderley, Shlomo Dubnov, and Philippe Depalle. Instrumental gestural mapping strategies as expressivity determinants in computer music performance. In *Kansei, The Technology of Emotion. Proceedings of the AIMI International Workshop*, pages 68–73, Genova, 1997.

23. Doug Van Nort, Marcelo M Wanderley, and Philippe Depalle. Mapping control structures for sound synthesis: Functional and topological perspectives. *Computer Music Journal*, 38(3):6–22, 2014.